ISJMS

ISSUE: 4
VOLUME: 2

IMAGE RECONSTRUCTION FOR HEAD LASER TOMOGRAPHY SYSTEM

Kafa Lazer Tomografi Sistemi İçin Görüntü Oluşturma Algoritması

Hüseyin Özgür Kazancı[1]
[1]Akdeniz University, Faculty of Engineering, Department of Biomedical Engineering

Date Submitted: 07.03.2016
Date Initiated: 05.09.2016

Kazanci HO. Image Reconstruction for Head Laser Tomography System ISJMS 2016;2(4): 51-55.

ABSTRACT

New hardware and image reconstruction algorithm for diffuse optical imaging (DOI) is presented in this work. Image reconstruction approach for new biomedical imaging device is presented. Primary-purpose laser scanner was used as a data acquisition unit for back-reflected laser light. It has one photodetector. One photodiode used with surface scanning process might be considered as a multi detector system. The photodiode, inside the laser scanner collects escaping photons from tissue surface, and can be evaluated as many photodetectors. The photodiode collects back reflected escaping photons from heterogeneous tissue or tissue like phantom media's each surface line pixel. Basically, solenoid mirror relay vibrates the laser pointer at the surface, in very short time interval. Back reflected laser light is collected by one photodiode. In this work, the non-contact laser scanning tomography device concept and simulative image reconstruction procedure is presented. Image reconstruction was done base on the blood dependent laser wavelength, which is 850 nm.

Key words: Diffuse Optical Imaging (DOI), Laser Data Acquisition, Image Reconstruction

ÖZET

Bu çalışmada yeni bir donanım ve bu donanımın yer aldığı diffüz optik görüntüleme sistemi için gerekli olan görüntü oluşturma algoritması sunulmaktadır. Biyomedikal optik görüntüleme aygıtı için gerekli olan görüntü oluşturma algoritması yaklaşımı aktarılmaktadır. Öncelikli amaçta veri toplama ünitesi olarak genel amaçlı lazer tarayıcı ünitesi geri yansıma geometrisinde çalışan diffüz optik tomografi cihazı olarak kullanıldı. Cihaz içerisinde, 1 adet fotodiyod fotodetektör bulundurmaktadır. İçerisinde 1 adet fotodiyod bulunduran lazer tarayıcı ünitesi içerisindeki tarayıcı ayna sayesinde doku yüzeyini tarayabilmektedir. Doku yüzeyindeki birçok piksel noktasını tarayabildiği için bu cihaz çoklu detektör yapısına sahip gibi düşünülebilir. Cihaz içerisindeki fotodiyod doku yüzeyinden dışarıya kaçan fotonları toplamaktadır. Cihaz tarama işlemi yapmasından dolayı da çoklu fotodetektör sistemine sahip olarak düşünülebilir. Fotodiyod, heterojen doku veya doku benzeri fantomun yüzeyindeki çizgisel hat boyunca yüzeyden kaçıp geri yansıyan fotonları toplamaktadır. Temel olarak solenoid ayna rölesi doku yüzeyinden belirli bir mesafede çok kısa zaman aralığında titreştirilerek doku yüzeyinin içerisinden geri yansıyan fotonlar toplanmaktadır. Geri yansıyan lazer ışığı ayna sayesinde fotodiyod üzerine düşürülmektedir. Bu çalışmada dokunmadan çalışacak olan lazer tarayıcı tomografi aygıt yapısı ve simulatif görüntü oluşturma prosedürü sunulmaktadır. Görüntü oluşturma algoritması izobastik olarak kana duyarlı dalga boyu olan 850 nm dalga boyuna bağlı olarak yazılmıştır.

Anahtar kelimeler: Diffüz Optik Görüntüleme, Lazer Veri Toplama, Görüntü Oluşturma.

INTRODUCTION

The concept of diffuse optical imaging (DOI) system is presented in this work. In general, DOI or diffuse optical tomography (DOT) systems collect back reflected escaping photons from tissue or tissue like phantom media by photodetectors, which are traditionally used at the tissue surface with fiber optic probes. Non-contact tomography could be an idea for image reconstruction procedure. Source and detector positions were determined. Photon fluence rate distributions were computed to build a forward model weight functions matrix. After building the forward model, the inverse problem is solved to recover the unknown properties of the tissue and reconstruct the images using various algorithms. Using a laser scanning device has two major advantages. Firstly, it is a non-contact medical imaging device. Secondly, each scanning point can be assumed as an independent photo detecting device such as a photodiode. Traditionally DOT devices require source and detector fibers to touch the tissue being examined. In general these devices are touching the tissue surface. Source and detection points, are fiber optic probes. Fiber optic probes are transmitting source and back-reflected detector laser light. This is good for soft tissues because soft tissues are taking the shape of rough imaging objects. On the contrary, if the imaging tissue is not soft, detectors cannot collect escaping photons from detection points, because detector points are lost. For these reasons devices can only be used for soft tissues. They can also be used in a non-contact mode but tissue buffers should be used in front of or around the tissue media such as intralipid. An example would be the breast imaging. Laser light is scattered and absorbed inside the tissue by cellular structures such as lipid membranes, cellular nucleus and organelles. Two of the important optical parameters are absorption and scattering coefficients. Absorption and scattering coefficients have been determined for different tissue types in literature [1-3].

Corresponding Author: Hüseyin Özgür Kazancı, Akdeniz University, Faculty of Engineering, Department of Biomedical Engineering
Email: ozgurkazanci@akdeniz.edu.tr

Three type of DOT devices are built based on the running procedure for research and medical application purposes. The first and the most basic type is the continuous wave diffuse optical tomography (CWDOT) systems [4]. The others are time resolved and frequency domain DOT systems. Building of the time resolved and frequency domain systems are too expensive. CWDOT systems are portable, photo-detecting units that have been fully integrated. Making a portable biomedical imaging device has been one of the goals for researchers. However, the basic theory and the philosophy should be deeply understood. Researchers have been working on DOT phenomena for almost three decades. The advantage of using low power laser comes with photon scattering and absorption physics which is a photon-tissue interaction case. Researchers have always been interested in using diffuse laser light for biomedical imaging purposes. DOT theory has previously been studied [5, 6].

CWDOT systems can also be divided into two branches depending on the imaging geometry. These are transmission through and back the reflected geometries. There is also a ring model, which combines both of them. Most of the continuous wave (CW) DOI breast devices are built as a ring model, which has both source and detector fiber optic probes at the ring surface [7-13]. DOI involves two important steps. These are data acquisition and image reconstruction processes. Data acquisition consists of electronic hardware and software instrumentation. Researchers have worked on instrumentation and image reconstruction models of DOI [14-16].

Researchers should model photon propagation inside the tissue. Photon migration defines the light distribution inside the imaging media. Each voxel inside the tissue is responsible for measured light intensity at the tissue surface. Diminished light intensity is the total product of the weight functions and delta absorption coefficient differences over homogeneous background media. Photon fluence rate distributions define these weight functions for each voxel. Theoretical physics approach or Monte Carlo (MC) simulation of photon tissue interactions calculate photon fluence rate distributions or deposited photon energies. Born or Rytov diffusion equation approximation of the radiative transport formula gives us information about how the photons distribute inside the homogeneous tissue. The other way is the MC simulation. Most of the researchers apply MC simulation methods to generate the pencil beams. After defining photon distributions, the next step is to generate weight functions between each source and detector positions. For each source and detector positions photon fluence rate distributions are calculated then multiplied to generate the banana weight functions. While building weight matrix, researchers presume the imaging tissue to be homogeneous media. For breast or brain imaging, they select tissue properties as homogeneous parameters. Breast tissue mostly consists of fat. For brain imaging, white and grey matters are the homogeneous background. These soft tissue's absorption and scattering coefficients constitute weight functions. Weight matrix is the forward model of the DOT imaging [17] – [24]. Depending on the source and detector positions, they build weight matrix correctly. They use fibre optic probes for source and detector positions. Fibre optic probes illuminate and collect back reflected laser light. DOI devices need source and detector fibers to touch the tissue being examined.

The second and important process is the inverse problem solution algorithm for image reconstruction. The unknowns are the absorption coefficient differences over homogeneous background. Inverse problem solution algorithms solve the linearized equation system [25-28]. If the forward model laser wavelength is blood dependent, the solution will be high blood volume voxels.

MATERIAL AND METHODS

Instrumentation

In generally, researchers use fiber optic optodes for DOT systems. Fiber optic source and detector cables carry the illuminating and back reflected light. Using an array of many optodes makes the DOT system more complex, and harder to carry. There is also a fixation problem. In this work, we developed a practical, easy to use and transport, portable CWDOT device. We presented the image reconstruction concept. Instead of traditional DOT devices, fiber optic probes were not used for source and detector positions. We chose a non-contact device model. We used a laser scanner to define the detector positions. Laser scanner is scanning the surface of the tissue. The laser scanner's forward mode biased photodiode collects escaping photons from tissue or tissue like phantom media. The modality has one laser source, which sends 850 nm wavelength laser inside the imaging media and, one photodiode inside the laser scanner device. The system has one data acquisition electronic main board which has a microcontroller, analog current input digital voltage output analog to a digital converter (ADC) chip with embedded integrator and required active-passive electronic elements. An industry partner has fabricated printed circuit board (PCB) of data acquisition unit. A laser trigger initialized the run. We have selected integrating switched capacitors by digital bits. In Fig 1A, we have shown the fabricated data acquisition unit. We have acquired data by USB serial communication cable via to PC. We have selected pic18f2550 [30] (Microchip, Boise US) microcontroller as a system chip. The key element of the system design is the DDC112 (Burr Brown, Dallas US) ADC integrated circuit (IC) with analog current to voltage integrator.

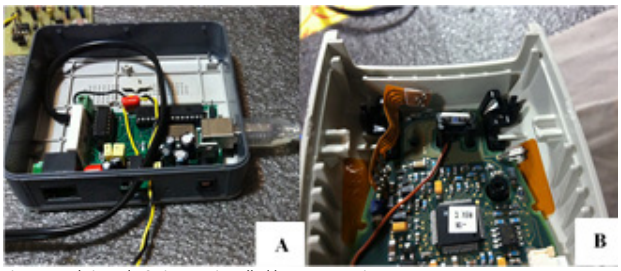


Figure 1: Fabricated PCB in A. Uninstalled laser scanner in B.

We have uninstalled the general purpose laser scanner. We have replaced the optic filter by 850 nm wavelength narrow band pass in front of the photodiode. In Fig. 1B, we have shown the uninstalled laser scanner. DDC112 ADC chip [29] has an internal integrator circuit with switched capacitors, connected from the output of the integrator to input. DDC112 gives a good opportunity to work on CW with the help of two integrators connected to the same photodiode channel. While one of the integrator stages is integrating the electrical charge, the other stage is connecting it to 20-bit resolution delta/sigma ADC circuit in the same chip. Dvalid signal is the data ready signal. Once the Dvalid signal pulls down, pic18f2550 microcontroller knows that the data is ready. The microcontroller sends 40 DCLK data clocks to DDC112 ADC chip to acquire digital data. The device has one laser source and one photodetector. While the laser scanner scans the specific line of tissue surface, it includes many pixel points. Thus, the system has many detector points. Depending on the image reconstruction strategy we could select detector numbers free criterion. The laser scanner has one mirror, which vibrates its solenoid inductance relay to illuminate source and collect back-reflected laser light in front of photodiode. The other laser source inside the scanner, runs at 650 nm wavelength to determine detector coordinates. This laser source is used to mark the detector coordinate points at the imaging surface. The real source is the 850 nm wavelength laser which is outside the laser scanner. One optic source and 36 detector coordinates are illustrated in Fig. 3. Once the detector positions are changed, deposited photon energies are changing between the source and detector positions. DOT problem consists of different steps. DOT requires multidisciplinary work. Electronic design and implantation is one of the system designs. The other and important part is the image reconstruction stage. Mathematical forward modeling of the proposed imaging modality was derived. The laser source position is constant; the laser scanner is rotated every five degree (5˚). Euclidian coordinate transformation was applied to generate required photon fluence rate distributions inside the imaging media. Coordinate transformation is ensuring the photon fluencies are calculated correctly. Deposited energies are changing depending on each source-detector matchups. Hence, there is only one optic source: detector positions are changed according to rotation angles. Two-dimensional (2D) MC photon-tissue interaction simulations were run for homogenous imaging media μ_a = 0.06 cm^{-1} absorption, μ_σ' = 12 cm^{-1} reduced scattering coefficients. Pencil beams were shown in Fig. 3A. Escaping diffuse reflectance vs. radius and deposited energy & photon fluence rates vs distance are presented in Fig. 3B and Fig. 3C. Rotation was done until the 360˚, radar imaging concept was considered. 5x5 cm x-y surface lengths were used for imaging geometry. X and y direction grids were divided into 25 grids. The 1.2 cm z direction was divided into 3 parts. This is 25x25x3 voxel

volumes. The source position is always constant. The detector positions were rotated according to the Euler coordinate transformation formula. Inclusion was put inside the imaging media for four different positions at the same depth layer. Inclusion positions were shown for 3rd z depth layer top view in Fig. 4. Reconstructed images were illustrated. The non-existent mathematical inverse problem solution algorithm requires that we recover the inclusion coordinates for DOT imaging problem. In literature, iterative, sub-space, and regularization methods have been tested for DOT imaging. In this work, we cannot calculate the exact weight functions for specific source and detector matchups. Because the device will scan the surface line, one source and many detectors. Photon fluence rate distributions were calculated but these were not directly used in image reconstruction process; because it includes more detector positions. There are 1 source and 36 detectors at each rotation. Translational weight matrix functions are shown in Fig. 3D and 3E. As long as the acquired data have a total combination of 36 possible source-detector couplings, the linearized equation system forward model weight matrix should also have these combinations. Traditional forward model weight matrixes have source-detector coupling rows and unknown absorption columns. However, it cannot be used for this device, hence one scan has more detector points. Each rotation has its own single perturbation measurement data, and total weight matrix functions according to the forward model. The perturbation equation is presented in Eq. (1). The weight matrix subscripts are source, detector, and voxel numbers, respectively. There are 25x25x3=1875 voxels for imaging medium. $\delta\mu_a$ is the unknown delta absorption differences over homogeneous background.

$$pert_i = \left[w_{1,1-1}\cdots w_{1,1-1875}\right]\times\begin{bmatrix}\delta\mu_{a1}\\ \delta\mu_{a2}\\ .\\ .\\ .\\ \delta\mu_{a1875}\end{bmatrix}+\left[w_{1,2-1}\cdots w_{1,2-1875}\right]\times\begin{bmatrix}\delta\mu_{a1}\\ \delta\mu_{a2}\\ .\\ .\\ .\\ \delta\mu_{a1875}\end{bmatrix}+\ldots+\left[w_{1,36-1}\cdots w_{1,36-1875}\right]\times\begin{bmatrix}\delta\mu_{a1}\\ \delta\mu_{a2}\\ .\\ .\\ .\\ \delta\mu_{a1875}\end{bmatrix}$$

$$pert_i = \left[\sum_{i=1}^{36} w_{1,i-1}\cdots\sum_{i=1}^{36} w_{1,i-1875}\right]\times\begin{bmatrix}\delta\mu_{a1}\\ \delta\mu_{a2}\\ .\\ .\\ .\\ \delta\mu_{a1875}\end{bmatrix}$$

Where w is the weight matrix, perti is the perturbation of ith detector measurement data. An Inverse problem solution algorithm was selected from one of the fast sub-space algorithms, which is also known as Conjugated Gradient (CG) method. Inclusions in four different locations were reconstructed.

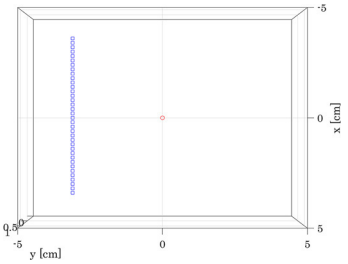


Figure 2: Source-detector placement

Reconstructed inclusions have noise. Inverse problem solutions are close to bigger weight coefficients' solutions. A basic laser scanner was considered to collect back the reflected laser light to the forward biased photodiode. Image reconstruction schema was presented. The device has one source and more detector coordinate positions at the same data acquisition time. While collecting laser light data, the device has a total of 36 detector positions. Detector numbers can be selected arbitrarily. Traditional DOI and near infrared spectroscopy (NIRS) devices have one source and one detector at the same time for one experimental measurement. In here, a total weight matrix term was used instead of a single weight matrix. This is one of the two important steps of forward model weight generation. The other is using Euler coordinate transformation.

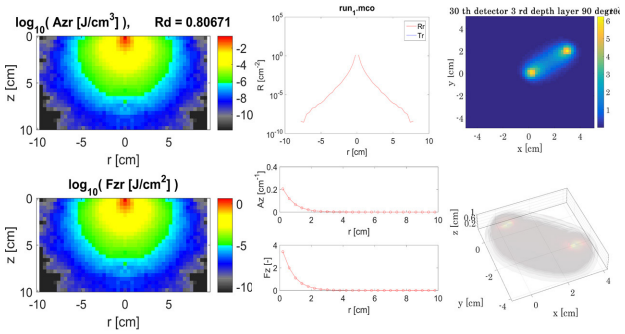


Figure 3: Pencil-beam photon fluence energy distributions over volume A. Escaping diffuse reflectance vs radius B. Photon fluence rates vs distance C. 90° rotation 30th detector 3rd depth layer photon fluence rates top-view D. 90° rotation 6th detector 3d banana weight matrix functions E.

One source at the center is motionless; the detector line is rotating around stable z-axis every five degree (5)˚ and collecting measurement data for each rotation. The purpose of applying the rotation process is to acquire more experimental measurement data at the same time. More data gives more voxel intersections. More intersections help to solve the inverse problem to recover high blood volume voxel inclusions. Weight matrix functions for each specific source and detector coupling were generated. Two dimensional (2D) Monte Carlo (MC) simulations were run and an MC output was used to generate the forward model weight functions. 2D MC simulation data were translated through three dimensional (3D) image reconstruction DOI platform. 2D MC simulation was run for r=26 and z=26 cylindrical coordinates. 3D DOI algorithm was realized for the 25x25x3 coordinate system. Imaging tissue was selected as homogenous one type media. Diffusing photons inside the tissue exhibits nonlinear equation model. It is generally converted to linear equation for the simplicity of the problem. Diffusing photons have the characteristic behavior of nuclear radiative transport equation. Radiation transport formula is linearized by the first Taylor term of Rytov or Born diffusion approximation. Image reconstruction requires the solution of the inverse problem. Inverse problem solution methods can be divided into three different groups. Iterative, subspace and regularization methods. The most famous iterative method is the algebraic reconstruction technique (ART) and simultaneous iterative reconstruction technique (SIRT). The most frequently used sub-space methods are singular value decomposition (SVD), truncated singular value decomposition (TSVD), conjugated gradient (CG), and truncated conjugated gradient (TCG) methods. The third method used for ill-posed linearized equation systems such as data with artifacts and noises, are known as regularization methods. The Tikhonov regularization method is the most known and used regularization technique for DOI devices [31].

RESULTS

In this work, the CG algorithm was selected to solve the linearized problem. CG algorithm is a fast method for seeing the results of the interested solution. Cubic inclusion was put into four different locations inside the homogenous tissue simulation model. Reconstructed images can be seen in Fig. 4. 2D MC photon-tissue interaction simulations were run for homogenous imaging media μ_α = 0.06 cm_{-1} absorption, μ_σ' = 12 cm^{-1} reduced scattering coefficient. Simulation phantom sizes are 5x5x1.2 cm. Four inclusion positions are 3.75 cm, 3.75 cm, 0.6 cm; 1.25 cm, 3.75 cm, 0.6 cm; 1.25 cm, 1.25 cm, 0.6 cm; 3.75 cm, 1.25 cm, 0.6 cm. The inclusion absorption coefficient was selected as μ_α = 0.066 cm^{-1}.

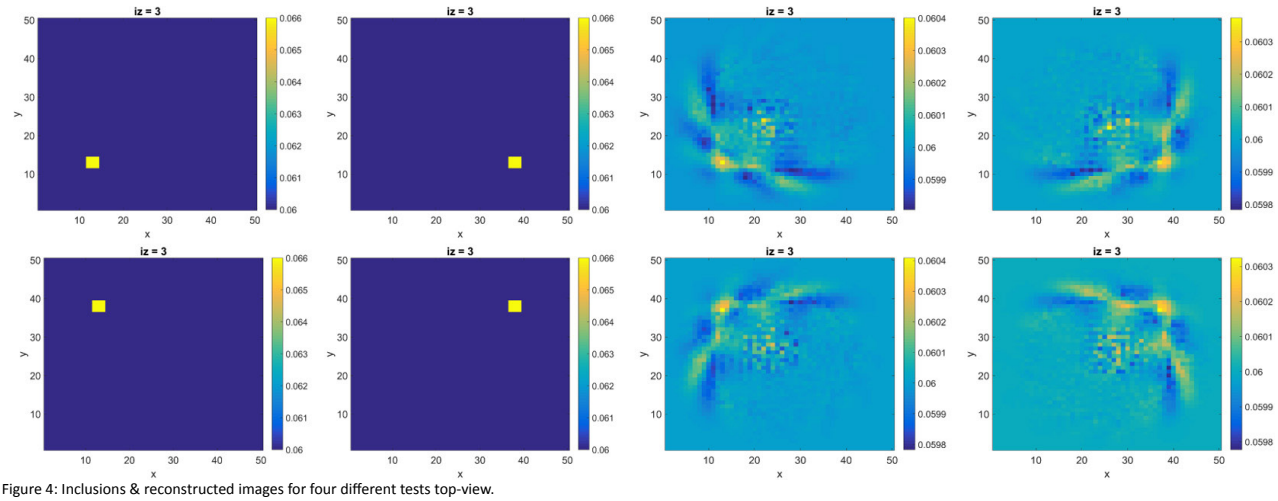


Figure 4: Inclusions & reconstructed images for four different tests top-view.

DISCUSSION

Four different inclusions were reconstructed successfully. Hence, photon energies are dense at the upper voxels; there are reconstructed image artefacts in those voxels, which are close to the surface. This is presumable and acceptable. In literature, there are many articles to equalize the importance factor of forward model weight matrix functions. One method is the depth compensation algorithm (DCA) which uses singular value decomposition (SVD) technique to equalize the importance of all tissue voxel weights. As long as the main purpose of this work is not the detailed analysis of image reconstruction algorithms, DCA method was not applied in here. This method changes weight functions therefore it effects inverse problem solutions. Reconstructed images have correct positions except with the noise problem because of the weight function differences for voxels. There is also source position noise. Hence, the system has only one source position; inverse problem solution algorithm has always some blurry noisy solution around the source. However, reconstructed images have correct localization. To support the future data acquisition novel design concept, forward model, and inverse problem solution results were proposed. Inverse problem solutions of DOT systems have blurry voxels, hence weight matrix functions haven't got equal importance. Voxels close to source and detector locations have always bigger advantage to be recovered. Real non-existence inverse problem solution algorithms are necessary to solve inverse problems unique. Improving the inverse problem solution is the key element.

CONCLUSIONS

Novel device and image reconstruction algorithm were implemented for DOI modality. A forward model weight matrix functions generation method was presented. Since the device is novel, geometric source and detector positions and forward model weight matrix generation procedures were initially designed and applied. 2D MC simulation data have been used to generate the forward model translational 3D weight matrix functions. Weight matrix functions were generated and illustrated in 2D top-view and 3D images. Weight matrix functions were used in image reconstruction process. High blood volume inclusion was put into four different positions for four different tests. Simulation perturbation data were generated and used inside the inverse problem solution algorithm. Inclusion was put in the same depth layer for different x and y coordinate positions. Recovered images were proposed.

REFERENCES

1. Wang LV, Wu H. Biomedical Optics: Principles and Imaging. New Jersey: Wiley; 2007. 362 p. http://doi:10.1002/9780470177013.ch1

2. González-Rodríguez P, Kim AD. Comparison of light scattering models for diffuse optical tomography. Opt Express. 2009;17(11):8756-8774. http://doi:10.1364/OE.17.008756

3. Ansari MA, et al. Diffuse Optical Tomography: Image Reconstruction and Verification. J Lasers Med Sci. 2014;5(1):13-18. http://dx.doi.org/10.1155/2015/286161

4. Siegel A, et al. Design and evaluation of a continuous-wave diffuse optical tomography system. Opt Express. 1999;4(8):287-298. http://10.1364/OE.4.000287

5. Yodh A, Chance B. Spectroscopy and imaging with diffusing light. Phys Today. 1995;48:34-40. http://dx.doi.org/10.1063/1.881445

6. Intes X, Chance B. Non-PET functional imaging techniques. Radiol Clin North Am. 2005;43(1):221-234. http://doi:10.1016/j.rcl.2004.07.002

7. Hielscher AH, et al. Near-infrared diffuse optical tomography. Dis Markers. 2002;18(5-6):313-337. http://dx.doi.org/10.1155/2002/164252

8. Lee K. Optical mammography: Diffuse optical imaging of breast cancer. Med. Phys. 2008;35(6), 2443-2451. doi:10.5306/wjco.v2.i1.64

9. Tromberg B, et al. Assessing the future of diffuse optical imaging technologies for breast cancer management. Mol. Imaging Biol. 2009;11(29):64-70. doi:10.1118/1.2919078

10. Ven Sv, et al. Diffuse Optical Tomography of the Breast: Initial Validation in Benign Cysts. Mol. Imaging Biol. 2009;11(2):64–70. doi:10.1007/s11307-008-0176-x

11. Flexman ML, et al. Digital optical tomography system for dynamic breast imaging. J Biomed Opt. 2011;16(7):076014. doi:10.1117/1.3599955

12. Patachia M, et al. Continuous wave diffuse optical tomography system tested on phantoms and animal tissues. Med Phys. 2015;67(2):412-422.

13. Zhang XF. Instrumentation in Diffuse Optical Imaging. Photonics. 2014;1(1):9-32. doi:10.3390/photonics1010009

14. Boas DA, et al. Diffuse optical imaging of brain activation: Approaches to optimizing image sensitivity, resolution, and accuracy. Neuroimage. 2004;23:275-288.

15.Hielscher AH. Optical tomographic imaging of small animals. Curr Opin Biotechnol. 2005;16:79-88. doi:10.1109/ISBI.2004.1398826

16. Kazanci HO, et al. Design and evaluation of a reflectance diffuse optical tomography system. Optical and Quantum Electronics. 2015;47(2):257-265. doi:10.1007/s11082-014-9910-6

17. Kazanci HO. Weight matrix analysis for back reflection continuous wave diffuse optical tomography (CWDOT) systems: translational method. Optical and Quantum Electronics. 2015;47(12):3847-3853. doi:10.1007/s11082-015-0252-9

18. Kazanci HO, et al. Investigation of Human Lung by Laser Tomography. El-Cezerî Journal of Science and Engineering. 2015;2(3):75-81.

19. Kazanci HO, et al. Depth Normalization Algorithm for Continuous Wave Reflectance Diffuse Optical Tomography System. El-Cezerî Journal of Science and Engineering. 2015;2(1):40-46.

20. Kazanci HO, et al. Mathematical method for diffuse optical tomography imaging: A Research Study. 2014;1(3):40-48.

21. Kazanci HO. Designing intact clinical head laser tomography system. In Proc. IEEE Medical Technologies National Conference (TIPTEKNO). 2015; 276-279. doi:10.1109/TIPTEKNO.2015.7374104

22. Kazanci HO. Development of coordinate definition algorithm for head laser tomography system. In Proc. IEEE Medical Technologies National Conference (TIPTEKNO). 2015; 280-283. doi:10.1109/TIPTEKNO.2015.7374105

23. Kazanci HO, Jacques SL. Diffuse light tomography to detect blood vessels using Tikhonov regularization. In Proc. SPIE - Saratov Fall Meetings SFM'15, Optical Technologies in Biophysics & Medicine XVIII. 2015;Saratov State University, Saratov, Russia.

24. Arridge SR. Methods in diffuse optical imaging. Philos Trans Phys Sci Eng. 2011;369(155):4558-4576. doi:10.1098/rsta.2011.0311

25. Arridge SR. Optical tomography in medical imaging. Inverse Problems. 1999; 15(2):41.

26. Arridge SR, Hebden JC. Optical imaging in medicine: II. Modelling and reconstruction. Phys Med Biol. 1997;42(5):841-53.

27. Hebden JC, et al. Optical imaging in medicine: I. Experimental techniques. Phys Med Biol. 1997;42(5):825-840.

28. Burr Brown Products and Texas Instruments, "Dual Current Input 20-bit analog to digital converter", DDC112 SBAS085B datasheet manual, Tucson AZ (2000) revised (2004).

29. Microchip Pic18f2550 datasheet manual, Chandler, AZ with wafer fabs in Tempe, AZ and Gresham, OR, 2004.

30. Cao N, et al. Image reconstruction for diffuse optical tomography using sparsity regularization and expectation-maximization algorithm. Opt Express. 2007;15(21):13695-13708.

31. Niu H, et al. Development of a compensation algorithm for accurate depth localization in diffuse optical tomography. Opt Lett. 2010;35(3):429-31. doi:10.1364/OL.35.000429

Conflict of Interest

The authors declare no conflict of interest.